



Available online at www.sciencedirect.com



International Journal of Pharmaceutics 280 (2004) 1–16

international
journal of
pharmaceutics

www.elsevier.com/locate/ijpharm

Freeze drying—principles and practice for successful scale-up to manufacturing

S.C. Tsinontides*, P. Rajniak, D. Pham, W.A. Hunke, J. Placek, S.D. Reynolds

Merck Research Laboratories, Merck & Co. Inc., Sunnystown Pike WP78-204, West Point, PA 19486, USA

Received 13 October 2003; received in revised form 9 April 2004; accepted 9 April 2004

Available online 25 June 2004

Abstract

Freeze Drying involves transfer of heat and mass to and from the product under preparation, respectively, thus it is necessary to scale these transport phenomena appropriately from pilot plant to manufacturing-scale units to maintain product quality attributes. In this manuscript we describe the principal approach and tools utilized to successfully transfer the lyophilization process of a labile pharmaceutical product from pilot plant to manufacturing. Based on pilot plant data, the lyophilization cycle was tested during limited scale-up trials in manufacturing to identify parameter set-point values and test process parameter ranges. The limited data from manufacturing were then used in a single-vial mathematical model to determine manufacturing lyophilizer heat transfer coefficients, and subsequently evaluate the cycle robustness at scale-up operating conditions. The lyophilization cycle was then successfully demonstrated at target parameter set-point values.

© 2004 Elsevier B.V. All rights reserved.

Keywords: Freeze drying; Lyophilization; Heat and mass transfer; Process scale-up; Pilot plant; Manufacturing; Pocket logger

1. Introduction

Lyophilization is commonly used in the pharmaceutical and biotechnology industries to improve the stability of formulations. The active pharmaceutical ingredient and accompanying excipients are first solubilized in a solvent (usually water), and the solution is rendered sterile by filtering it through 0.2 µm or equivalent sterilizing grade filters. The sterilized solution is filled into vials, then loaded into a lyophilizer where the solution is frozen, and subsequently heated

at very low pressure to sublime the solvent and remove it from the formulation. Once the water is removed, the product vials are sealed under vacuum or an inert gas head space (i.e., N₂, Ar). The resulting highly porous cake has low moisture content and can be stored over extended periods of time at the designated storage conditions until its intended use.

Over the past few decades, the investigation of the fundamental physical phenomena occurring in each step of freeze drying has led to producing stable and elegant freeze-dried pharmaceutical dosage forms. A comprehensive review of the principles and practice of freeze drying was published by Nail and Gatlin (1992). Extensive work in studying the physical chemistry, and transport phenomena during freezing and primary drying (MacKenzie, 1975; Pikal et al., 1983a, 1984, 1990; Pikal, 1985, 1990a,b; Franks, 1990) paved the way for designing appropriate formu-

Abbreviations: AVG, average value; N, number of samples tested to determine average value

* Corresponding author. Tel.: +1 215 652 2651; fax: +1 215 652 4088.

E-mail address: stelios_tsinontides@merck.com
(S.C. Tsinontides).

Nomenclature

A, B	constants in Eq. (3)—values taken from Pikal (1985) defined in Table 4
C, D	constants in Eq. (2) defined in Table 4
$D_{\text{win,e}}$	Effective pore diffusivity in the cake defined in Table 3 (m ² /s)
h	overall heat transfer coefficient as defined in Eqs. (1) and (4) , defined in Table 4 (W/m ² K)
h_c	heat transfer coefficient by direct conduction between shelf and glass vial, defined in Eq. (2)
h_r	heat transfer coefficient by radiative heat from upper and bottom shelves, defined in Eq. (2)
h_g	heat transfer coefficient by convective heat transfer from bottom shelf, defined in Eq. (3)
k_{des}	Rate constant of desorption step defined in Table 3 (s ⁻¹)
K, a_{max}	Langmuir equilibrium parameters defined in Table 3
P	chamber pressure (Pa)
T	temperature (°C)
T_{ice}	ice temperature is the maximum temperature of frozen amorphous solution during primary drying (°C)
T_c	collapse temperature of an amorphous system; considered to be equal to T_g' for design and scale-up purposes (°C)
T_g'	glass transition temperature of an amorphous system defined in Table 3 (°C)
$T_{\text{g,solid}}, K_{\text{mix}}$	Gordon–Taylor parameters defined in Table 3

Greek symbols

λ_{cake}	effective thermal conductivity of the cake defined in Table 3 (W/m K)
-------------------------	---

lations and lyophilization cycles. At the same time, considerable advancements in modelling of freeze drying have yielded mathematical models to describe the dynamic behavior of primary and secondary drying of pharmaceutical solutes ([Liapis and Bruttini, 1994, 1995; Liapis et al., 1996; Sadikoglu and Liapis, 1997](#)). The recent advancements in lyophilization technology notwithstanding, issues of scale-up have attracted limited attention. Scale-up is a critical step that determines timely product commercialization, and regulatory guidances expect that the manufacturing process be demonstrated at manufacturing-scale to produce uniform product within the batch, with desired physical and chemical attributes ([FDA Guideline, 1987](#)).

This manuscript presents a methodology utilized to successfully scale-up the lyophilization cycle of a labile pharmaceutical formulation from pilot plant to manufacturing. A series of scale-up runs were executed to evaluate a proposed process window of operation. Data from the scale-up runs were then used in a mathematical model to evaluate the robustness of the lyophilization cycle to likely operating condi-

tions. Based on the collective results from experiments and model simulations, the final lyophilizer set points and window of operation were determined. The process parameter set-point values were then successfully demonstrated in a final run.

2. Experimental approach

The lyophilization cycle was developed from studies in a laboratory-scale lyophilizer¹. Once the set points were determined (e.g., temperature, pressure, duration of drying steps at different temperatures, rate of temperature increase), the cycle robustness was evaluated by varying temperature and pressure around set points to establish operating ranges. The optimized cycle was then applied successfully to a pilot plant lyophilizer with the manufacture of clinical and stability batches with no adjustment to cycle set-point values based on comparable lyophilizer dimensions.

¹ VirTis Benchmark 1000 lyophilizer.

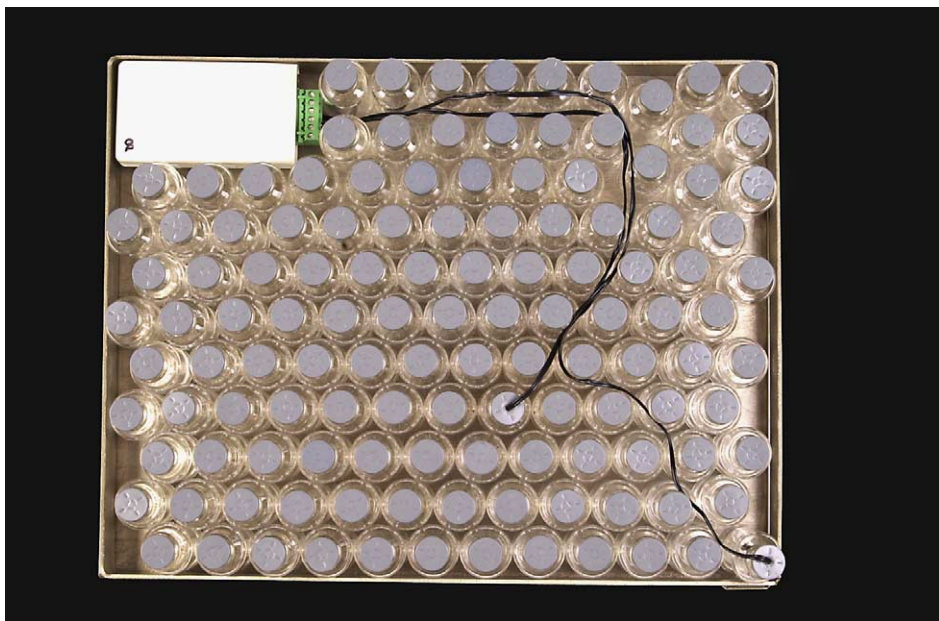


Fig. 1. Representation of Pocket Logger placement in a frame to monitor product temperature of vials at different locations.

Upon transferring the process to Manufacturing, the development scale-up batches to demonstrate the cycle were limited due to plant availability and active raw material supplies. Initially, a small number of vials containing the formulation were placed into the lyophilizers among placebo vials during the shake-down and qualification of the manufacturing lyophilizers. A placebo formulation made of lactose and sucrose had been developed to match the formulation physical properties by closely matching T_g' and solid content ($T_g' = -25^\circ\text{C}$, 25% solids content).

During the placebo trials Pocket Loggers² were evaluated to monitor product temperature during lyophilization. Pocket Loggers are used widely to monitor temperature, humidity or other variables during material shipment and other applications. In all of our studies we used Pocket Logger model XR-440 (size 12.0 cm × 6.1 cm × 2.3 cm), which was quoted to have a wide range of operating temperature (−40 to 60 °C), and good accuracy ($\pm 0.15^\circ\text{C}$). The pocket logger was tested at the extreme conditions of the

lyophilization cycle and its operation was found to be robust. Its small size and portability allowed its use to probe vials at many locations on different shelves without influencing the rate of heat transfer to the product being monitored. Fig. 1 demonstrates how the Pocket Logger was placed among filled vials in a tray to monitor product temperature at different locations inside the lyophilizers. Fig. 2 shows the placement of the thermistor inside a product vial. Thermistors were placed in product vials carefully ~3 mm above vial bottom and centered for consistency of measurement in the different vials and studies. The probed vials were frozen outside the lyophilizer at a similar rate as the product to secure the probe in place. The pocket loggers and probed vials were then placed into designated locations inside the frames just prior to loading the frames into the lyophilizer.

The accuracy of the thermistor probe used on the Pocket Logger was evaluated against thermocouple probes used during development in laboratory-scale lyophilizers (thickness of thermocouple probe was ~0.25 mm). Fig. 3 compares the readings of thermistor and thermocouple probes in a laboratory-scale lyophilizer study. The two probe readings were slightly different toward the end of primary drying with the thermistor probe indicating a faster rise of

² Pocket logger is a product of Pace Scientific Inc. In our studies we used Pocket logger model XR-440, and temperature thermistor model PT-907.



Fig. 2. Location of the thermistor probe inside a product vial.

Table 1
Timeframe of technical transfer activities in manufacturing

Time frame	Activity
Months 0–11	Placebo runs; vials containing active formulation dispersed among placebo vials for testing lyophilization equipment operation Trial 1: preliminary scale-up run (1/2 placebo 1/2 active vials)
Month 15	Trial 2: scale-up #2 Trial 3: scale-up #3
Month 18	Trial 4: demonstration run

product temperature than the thermocouple probe. The difference in the readings is attributed to the probe sizes. The thermistor probe diameter is large and the temperature reading represents that of a larger area around it, hence somewhat less accurate in measuring local temperature than a thermocouple. The somewhat lower sensitivity of the thermistor to measure local temperature was taken into account when interpreting data generated at the manufacturing scale.

The technology transfer process for scale-up was carried out in three phases, as shown in Table 1. The

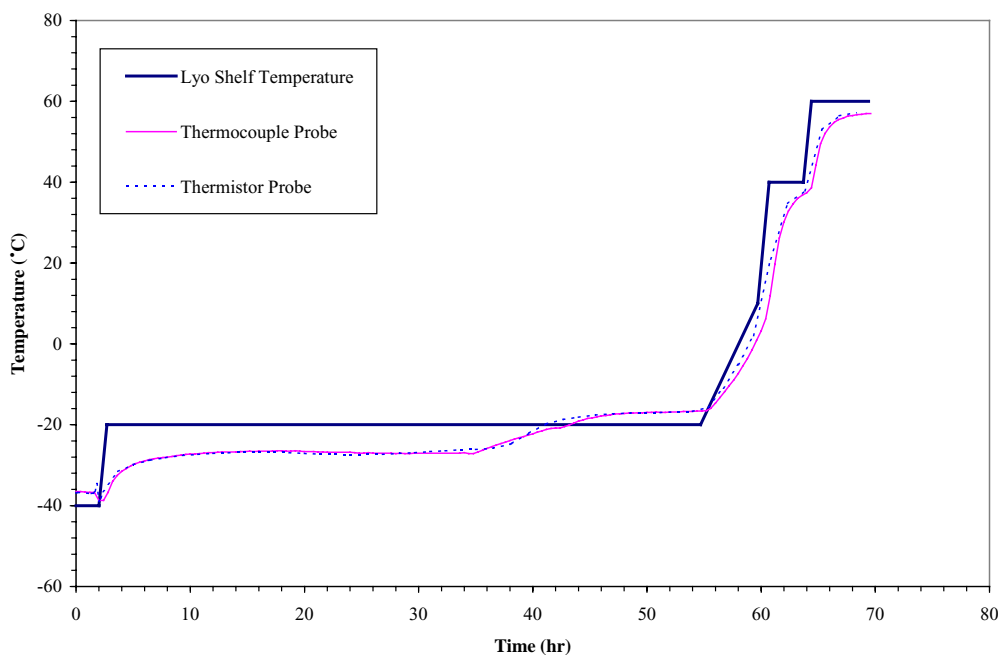


Fig. 3. Product temperature during a lyophilization cycle measured by a thermocouple probe (~0.25 mm diameter) and a data logger thermistor probe (~2.85 mm diameter).

Table 2
Lyophilization parameters during the technology transfer batches in manufacturing

Parameters	Preliminary scale-up set-point values	Trial 2 Set-point values	Trial 3 Set-point values	Trial 4 Demonstration run
Primary drying				
Temperature (°C)	–21	–22	–20	–20
Pressure (Pa)	11.0	9.5	12.5	11.0
Secondary drying				
Temperature (°C)	40	39	41	40
	60	59	61	60
Pressure (Pa)	5.0	3.5	6.5	5.0

first phase consisted of performing placebo runs followed with an initial trial (Trial 1) to identify the preliminary lyophilization cycle set points at manufacturing scale, shown in Table 2. In the second phase (Trials 2 and 3), the set point parameters were challenged to determine a process operating window and the final scale-up set-point values. In Trial 2, the pressure and shelf temperature set points were held below target to test conditions of low heat transfer to the product. In Trial 3, the cycle was tested under aggressive heat transfer conditions. The lyophilization cycle ramps and duration of the steps were not varied. Relatively small changes in the operating conditions ($\pm 1^{\circ}\text{C}$ and

$\pm 1.5 \text{ Pa}$) had significant impact on the process because of high solid content in the product and consequently high resistance of the dried cake to the vapor flow. The results from Trials 2 and 3 were not sufficient to readily identify final lyophilization parameter set points, hence a theoretical model was employed to evaluate lyophilization cycle robustness at manufacturing scale and assist in determining the appropriate parameter set points. The final parameter set points, shown in Table 2, were demonstrated in Trial 4. Fig. 4 shows the locations of product vials with thermistors during the scale-up runs. Vials were probed throughout the cabinet to obtain a comprehensive picture of product drying within a lyophilization load. Vials at the center and inside the shelf and around shelf periphery with and without contact with metal frames were probed. Moisture testing was done on vials from similar locations at the end of lyophilization.

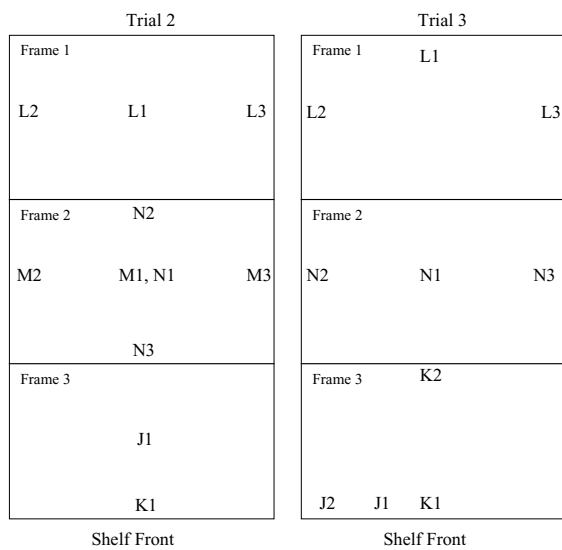


Fig. 4. Top view of thermistor and moisture mapping locations of product vials in the lyophilizer for Trials 2 and 3 (locations are not limited to a single shelf).

3. Theoretical approach

Because of the limited availability of experimental data at manufacturing scale, a theoretical model predicting primary drying in a single vial (Rajniak et al., 1999) was used to fully explore the robustness of the lyophilization cycle and to set final parameter set points. Model equations and boundary conditions, which include energy balances in the frozen and dried regions of the cake, mass balances in the dried cake and at the moving interface, and adsorption–desorption equilibrium and rate expressions, are found elsewhere (Rajniak et al., 1999, 2000), and are based on those developed by Liapis and coworkers (Liapis and Bruttini, 1994, 1995; Liapis et al., 1996; Sadikoglu and Liapis, 1997). The

Table 3
Model parameter values

Parameter description	Value
Effective thermal Conductivity of the cake, λ_{cake} (W/m K)	0.04
Effective pore diffusivity in the cake, $D_{\text{win,e}}$ (m ² /s)	0.0011
Langmuir equilibrium parameters	$K = 355$, $a_{\text{max}} = 1256$ mole/m ³
Rate constant of desorption step, k_{des} (s ⁻¹)	3.3×10^{-5}
Gordon–Taylor parameters	$T_{\text{g,solid}} = 110$ °C, $K_{\text{mix}} = 5.6$
Glass transition temperature, T'_{g} (°C)	–25

model has a number of parameters specific to product physical properties, product package configuration, and lyophilizer properties, and were calculated or estimated based on readily available product/process information. The values of these parameters are shown in Tables 3 and 4. The effective pore diffusivity for water transport in the dried cake and the overall heat transfer coefficient between the shelf and bottom of the vial were first obtained by fitting the model predictions to laboratory experimental data. It was assumed that the effective pore diffusivity would not change upon scale-up to a manufacturing lyophilizer. The assumption follows from the equivalent freezing step in all cycles and consequently the same structure of the frozen and dried product was expected. However, it was expected that heat transfer coefficients could vary among different units, as a result of different lyophilization design and size. Therefore, the scale-up data were used to determine heat transfer coefficients for modeling primary drying at the manufacturing units. The overall heat transfer coefficient between the product and the shelf, h , was expressed in the form proposed by [Pikal \(1985\)](#), as the sum of three contributing factors:

$$h = h_c + h_r + h_g \quad (1)$$

h_c denotes heat transfer conduction to the product from the shelf through the glass vial/shelf contact points, h_r denotes the radiative heat from the top and bottom

shelves, and h_g the convective heat transfer from the bottom shelf to the vial via the gas located between vial bottom and shelf. The first two contributions are independent of operating pressure, and the combined contribution of the two routes of heat transfer was assumed to vary linearly with shelf temperature in the limited window of temperatures considered as follows ([Tsinontides et al., 2001](#)):

$$h_c + h_r = C + DT \quad (2)$$

T is the absolute temperature of the shelf, and C and D are empirical constants specific to the vial/shelf configuration. The empirical relation (2) is used to express the temperature dependence of the “fictitious” radiation heat transfer coefficient h_r (based on the linear temperature driving force assumption; [Peters and Timmerhaus, 1981](#)). The gas contribution of heat transfer coefficient, h_g , is dependent on the operating chamber pressure. h_g is increasing with increasing pressure, and its form was adopted from [Pikal \(1985\)](#).

$$h_g = \frac{AP}{1 + BP} \quad (3)$$

The value of constant A is not specific to the vial/shelf configuration, but the value of B is, and values of A and B for tubing and molded vials are found in [Pikal \(1985\)](#). Using Eqs. (2) and (3), the heat transfer coefficient takes the following expression in terms of the independent operating variables, shelf temperature

Table 4
Heat transfer coefficients for manufacturing lyophilizers

Trial (#)	Shelf temperature (°C)	Chamber pressure (Pa)	Constant C (W/m ² K)	Constant D (W/m ² K ²)	Heat transfer coefficient ^a , h (W/m ² K)
2	–22	9.5	–267.4	1.08	11.5
3	–20	11.5	–267.4	1.08	15.0

^a Calculated from Eq. (4) using $A = 1.04$ W/m² K Pa and $B = 0.027$ Pa^{–1} ([Pikal, 1985](#)).

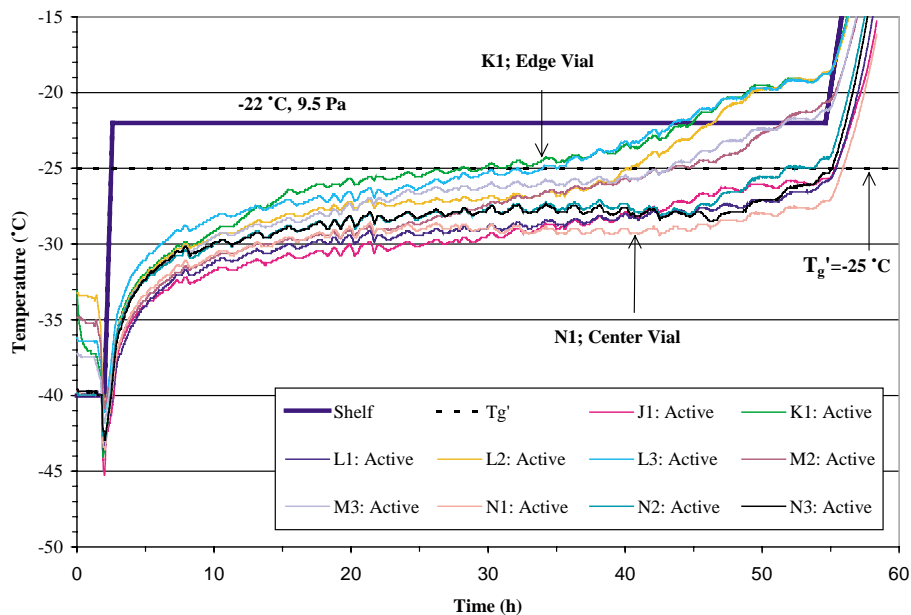


Fig. 5. Pocket logger thermistor (product) temperature during primary drying for Trial 2 in manufacturing at conservative primary drying conditions.

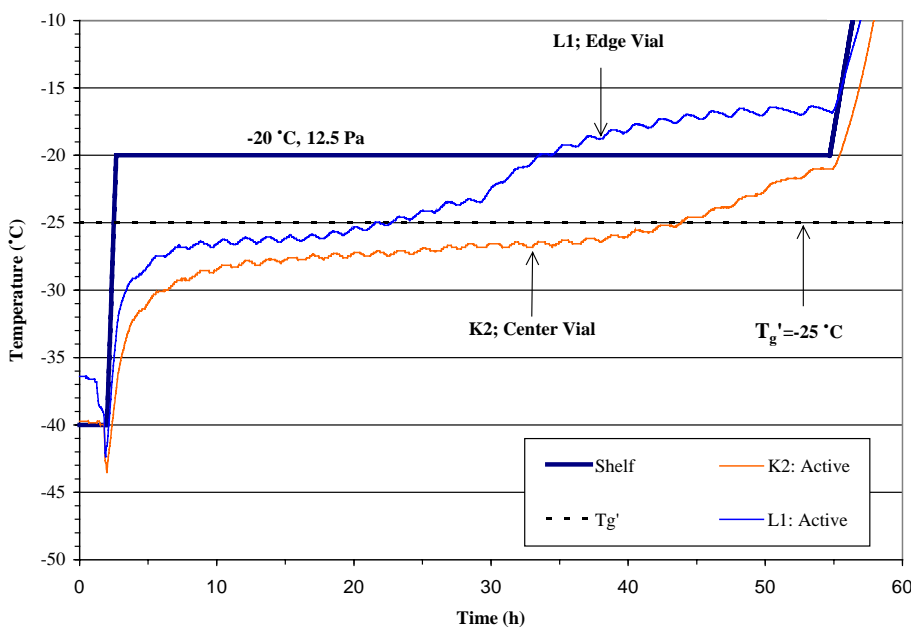


Fig. 6. Pocket logger thermistor (product) temperature during primary drying for Trial 3 in manufacturing at aggressive primary drying conditions.

and chamber pressure.

$$h = C + DT + \frac{AP}{1 + BP} \quad (4)$$

Eq. (4) contains four constants whose evaluation requires, in principle, at least four experiments at different operating conditions. However, in the present case, only two experiments were performed. Since constants *A* and *B* are dependent on the operating pressure and vial type and not as much on the properties of the lyophilizer shelves, their respective values were borrowed from [Pikal \(1985\)](#) and listed in [Table 4](#). The values of constants *C* and *D* were then determined by fitting the model predictions to experimental temperature transient of centered vials from Trials #2 and #3 (shown in [Figs. 5 and 6](#)). [Table 4](#) shows the calculated overall heat transfer coefficients at the operating conditions of Trial 2 and 3. As expected, at the more aggressive conditions (Trial 3), the overall effective heat transfer coefficient is higher (15.0 versus 11.5 W/m² K).

4. Results and discussion

4.1. Experimental results

The pilot plant lyophilization cycle is shown in [Fig. 3](#). Primary drying was conducted at -20 °C and 11.0 Pa, and secondary drying at 40 and 60 °C with pressure held at 5.0 Pa. The final product was demonstrated to have desired physical and chemical attributes (i.e., white to off-white cake appearance, moisture content of less than 2.5% (w/w), low levels of degradates) in the pilot plant lyophilizer; hence the cycle was determined to be appropriate for scale-up. The first scale-up batch (Trial 1) was conducted using the pilot plant demonstrated cycle set points. This was the first time a manufacturing lyophilizer was run with significant amount of product in the lyophilizer (1/2 of the lyophilizer had product and 1/2 had placebo formulation). The final product attributes were satisfactory, and upon review of the temperature trends of product vials, the preliminary set points of the lyophilization cycle were set, shown in [Table 2](#). The primary drying set-point temperature was decreased from -20 to -21 °C, but the other set points were not changed. Therefore, Trials 2 and 3

were conducted with primary drying at ±1 °C from -21 °C and ±1.5 Pa from respective pressure set points.

[Figs. 5 and 6](#) show primary drying temperature profiles of product vials from Trials 2 and 3, respectively (probe locations shown in [Fig. 4](#)). The conditions of primary drying and the formulation glass transition temperature, *T*_g' (-25 °C), are shown on the figures. [Fig. 5](#) shows that the product inside the manufacturing lyophilizer dried at two generally distinct rates. Vials in the interior of the shelves dried slower than vials close to the shelf periphery (edge vials). The profiles for center and edge vials are marked in [Fig. 5](#) (N1 and K1 for center and edge, respectively) with the remaining vials drying at intermediate rates. The marked variation in the product temperature transients, and hence apparent product drying rates, were typical in all trials and depended mostly on vial location on a shelf. [Fig. 6](#) and subsequent figures ([Figs. 7, 12–14](#)) show representative center and edge vial product temperature trends to demonstrate the range of drying rates within a lyophilizer. The variability of temperature transients (and hence of drying rates) during primary drying within a lyophilization load underlines the importance of spatial variability of heat transfer in large units. A lyophilization cycle can not be too aggressive because product at the periphery of a lyophilizer shelf could collapse due to aggressive heating (by melting the frozen solution), nor too conservative because product at shelf centers could collapse upon increasing shelf temperature due to incomplete primary drying.

The thermal results in [Figs. 5 and 6](#), along with the physical appearance and moisture results of the final product ([Fig. 8](#)) showed that the lower temperature and pressure during primary drying in Trial 2 resulted in some minor product partial collapse upon increasing shelf temperature. Approximately 5% of product vials in Trial 2, predominantly located near shelf centers, had signs of frozen solution melt at the bottom center of the cakes. The minor partial collapse was evident by a different color and texture, crescent-shaped, area at the lower part of cakes. The recorded temperature of center vials (e.g., vial N1 in [Fig. 5](#)) showed that the product located close to shelf centers did not complete primary drying. Several thermistors showed product temperature at or below the glass transition tempera-

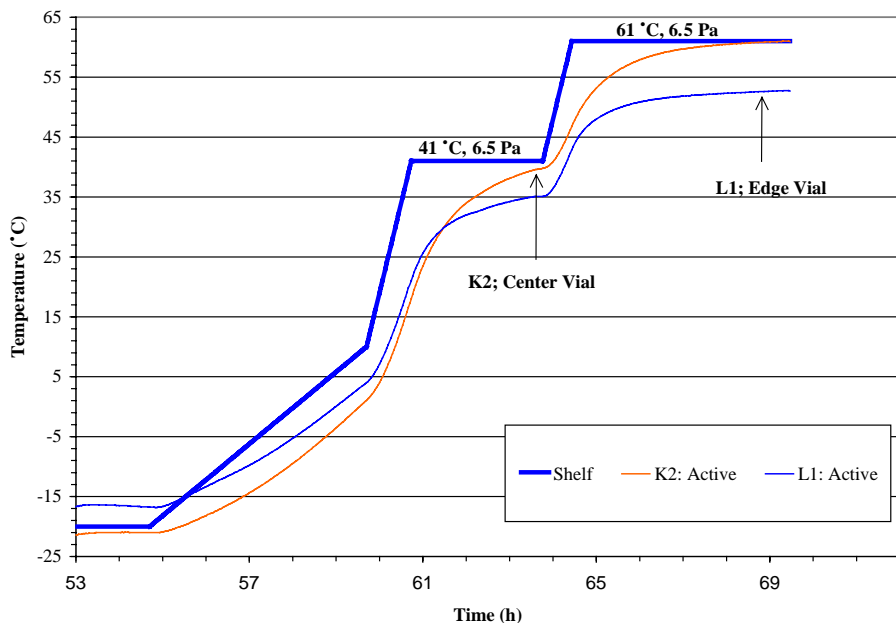


Fig. 7. Pocket logger thermistor (product) temperature during secondary drying for Trial 3 in manufacturing at aggressive secondary drying conditions.

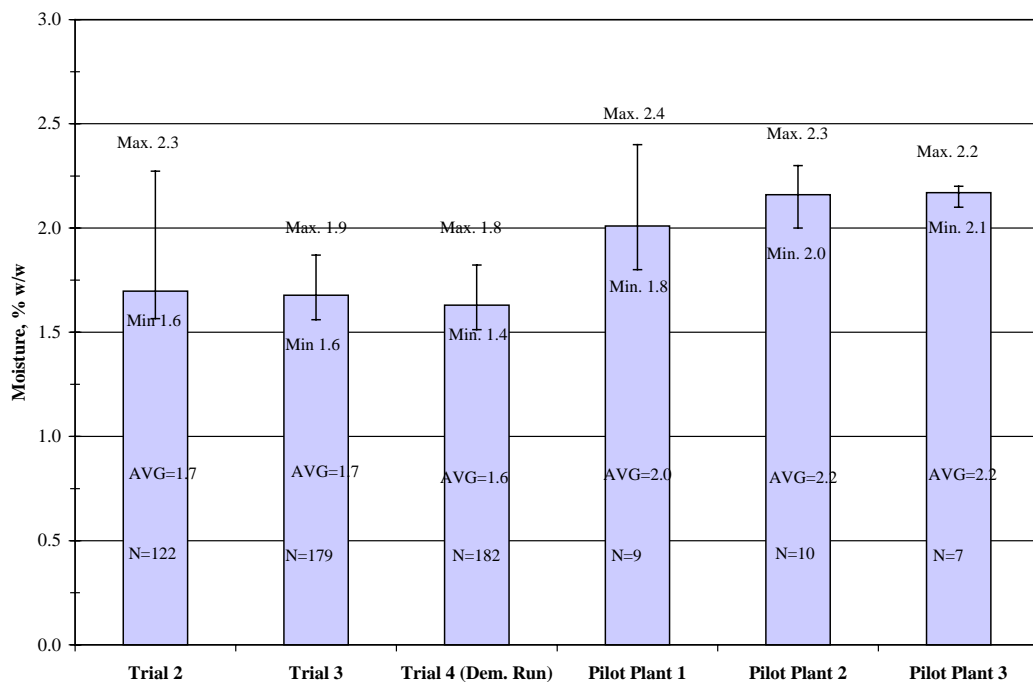


Fig. 8. Final product moisture in manufacturing scale-up (Trials 2–4) and pilot plant batches.

ture of the product,³ T'_g , at the end of the primary drying step (center vials in **Fig. 5**). If the temperature of the product is much lower than shelf temperature and below T'_g , then the sublimation of water was likely not complete in the entire cake. Increase of shelf temperature to proceed to secondary drying caused melting of portions of frozen solutions still undergoing sublimation. The location of the collapsed region at the bottom center of the cake was indicative of incomplete primary drying. Partial collapse of cakes at the upper and outer surfaces is characteristic of aggressive heating. In Trial 3 all product vials completed primary drying before the end of step, as demonstrated in **Fig. 6**. The recorded product temperature at all locations spanning from shelf centers (vial K2) to shelf edges (vial L1) were well above T'_g and close to the shelf temperature by end of primary drying step.

Fig. 7 shows the respective recorded temperatures of product at center and edge vials during secondary drying in Trial 3. As expected, similar variability of heat transfer within the lyophilizer shelves was observed at the secondary drying temperatures. The vials at shelf centers approached shelf temperatures (more effectively heated), but vials at the shelf periphery remained somewhat at lower temperature. The impact of secondary drying conditions on the product was determined based on the final moisture results, shown in **Fig. 8**. **Fig. 8** shows the average moisture (AVG), the number of samples tested (N), and range of moisture values for each scale-up and pivotal pilot plant batches. The average moisture results of scale-up batches were comparable, ranging between 1.6 and 1.7%. The minor partial collapse observed in ~5% of product in Trial 2 did not affect the average moisture value due to the larger number of vials tested. However, the limited number of partially collapsed product caused greater variability in moisture values. Overall, the moisture of product from manufacturing was lower than that from pilot plant (~1.6% compared to ~2.1%). Secondary drying conditions for batches in the pilot plant and manufacturing were very similar, thus product from both scales was expected to have similar moisture content. The difference is attributed to the different heat

transfer characteristics of the lyophilization units, an issue addressed later in the manuscript.

4.2. Theoretical results—lyophilization cycle robustness evaluation

The primary drying set points could not be readily determined because of product partial collapse observed in Trial 2. Availability of manufacturing time and of large amounts of costly materials to continue scale-up studies was limited, and the determination of primary drying set points could not be done experimentally. Furthermore, the shelf temperature of manufacturing lyophilizers oscillated around the set point during primary drying (evident by the measured product temperatures in **Figs. 5 and 6**). Hence, the available experimental data were incorporated into a mathematical model to evaluate lyophilization cycle robustness and determine final parameter set points.

Fig. 9 shows the ice temperature (frozen solution temperature) trend during primary drying at the experimental conditions of scale-up Trials 2 and 3. The simulation determines the increase of ice temperature and the duration of primary drying for a given target fill volume (height of the frozen solution). Collapse is predicted if the ice temperature exceeds the collapse temperature during primary drying, or the predicted primary drying duration exceeds the actual duration of the step used in manufacturing. The simulations for Trial 3 conditions showed that primary drying was completed successfully with maximum ice temperature of -26.2°C in 42.9 h, less than the experimental allocated time of 52 h. On the contrary, the simulations for Trial 2 conditions predicted a maximum ice temperature of -28.4°C after 52.4 h. The results in **Fig. 9** are in agreement with the experimental product temperature trends in **Figs. 5 and 6**, which showed that primary drying was not completed in Trial 2, and thus the limited amount of collapsed product and high product moisture values.

Fig. 10 shows the ice temperature trend during primary drying at the Trial 3 operating conditions. The amplitude and frequency of shelf temperature oscillations were closely matched to those observed during manufacturing with temperature oscillating $+1.3^{\circ}\text{C}/-0.6^{\circ}\text{C}$ from set-point value at a frequency of $\sim 0.6\text{ h}^{-1}$. The oscillations shifted the average shelf temperature to a slightly higher value from set-point

³ The collapse temperature, T_c , is usually determined to be slightly higher than the T'_g of the frozen solution. For process development considerations, a conservative approach has been adopted to consider T_c equal to T'_g .

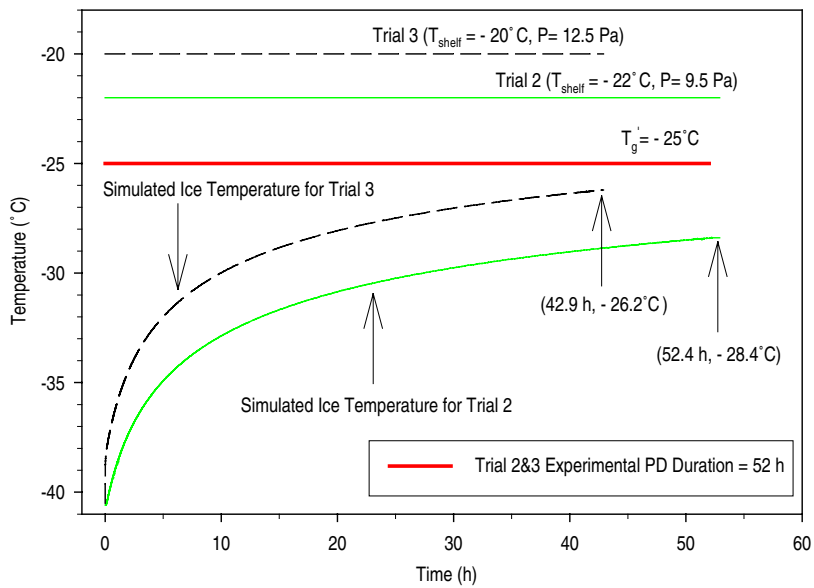


Fig. 9. Simulations of primary drying duration and frozen solution temperature (ice temperature), T_{ice} , for Trials 2 and 3.

making Trial 3 conditions worst-case scenario to simulate. The predicted ice temperature oscillations in Fig. 10 matched closely the experimental measurements of product oscillations in Figs. 5 and 6. The frozen product temperature oscillated at smaller am-

plitude than shelf temperature as a result of the heat transfer resistance limitations. Furthermore, as shown in Fig. 10 the predicted duration of primary drying with the oscillations (42.0 h) was smaller than without the oscillations (42.9 h) due to the slight upward

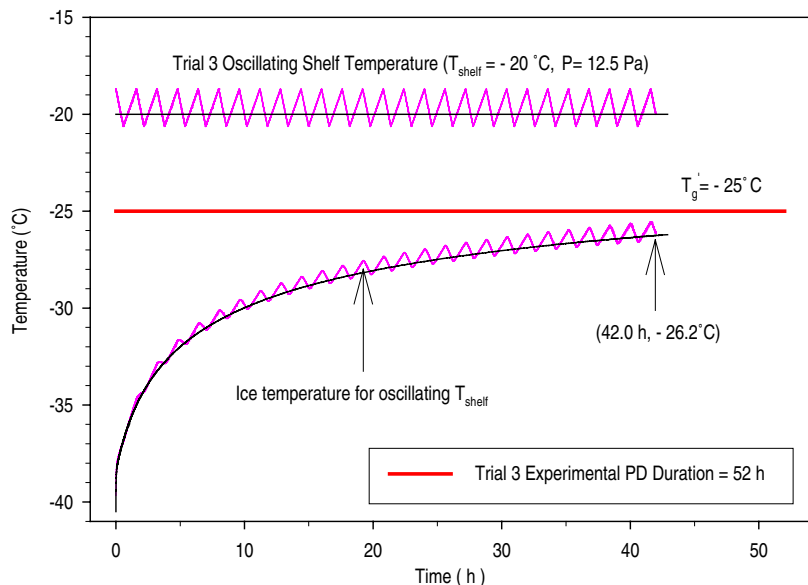


Fig. 10. Evaluation of primary drying robustness with oscillating shelf temperature for Trial 3.

shift of the averaged shelf temperature. The maximum ice temperature with the oscillations present was -25.5°C , and thus primary drying was expected to be completed without affecting product quality attributes.

Upon a complete evaluation of all process manufacturing data from scale-up trials, the solution target fill volume was decreased by $\sim 2\%$ (from 5.9 to 5.8 ml). However, the lyophilization cycle set points were tested at the scale-up trials' target fill volume to simulate worst-case scenario in terms of filling capability. Furthermore, primary drying was simulated with shelf oscillations at extreme conditions of operation. **Fig. 11** compares the results of such simulations to those at the final primary drying set points of -20°C and 11.0 Pa. The top curve corresponds to a shelf temperature oscillation at -19°C with pressure setting at 12.5 Pa. Primary drying duration at such aggressive heat transfer conditions was predicted to be only 38.5 h with frozen solution temperature reaching -24.9°C . Operation at this condition would be risky with possibility that some limited number of product vials could show partial collapse. This condition was thus considered the upper bound of the operating range for temperature and pressure during primary drying. The bottom curve corresponds to a shelf tem-

perature oscillation at -21°C with pressure setting at 9.5 Pa. Primary drying duration at these conservative heat transfer conditions was predicted to be 46.7 h with maximum frozen solution temperature reaching -27.0°C . At these conditions, the duration of primary drying was well within the actual set duration of 52 h, thus considered to be in the safe operating window. The middle curve predicted the duration of primary drying and maximum ice temperature at the proposed operating conditions for primary drying, -20°C and 11.0 Pa. Primary drying was predicted to require about 42.3 h with maximum ice temperature reaching -25.9°C , below the maximum allowable temperature of -25°C . Additional simulations were performed at different target fills. In all three cases, the duration of primary drying was predicted to be about ~ 1 h shorter with an ice temperature decrease of $\sim 0.1\text{--}0.2^{\circ}\text{C}$ at the target fill volume of 5.8 ml.

4.3. Final lyophilization cycle demonstration in manufacturing

Based on the experimental data and theoretical predictions, the primary drying set points were set to -20°C and 11.0 Pa. These conditions were robust to likely deviations from operating set points ($\pm 1^{\circ}\text{C}$;

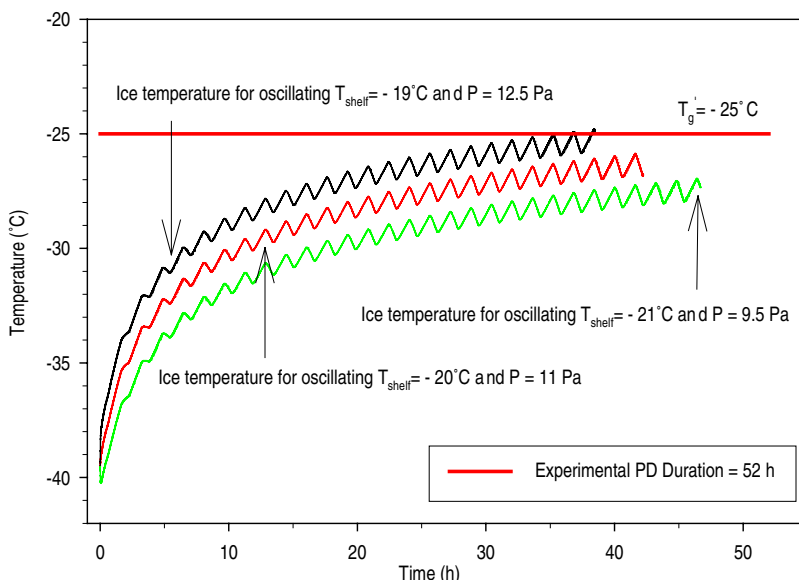


Fig. 11. Evaluation of primary drying robustness at different oscillating shelf temperatures and chamber pressures.

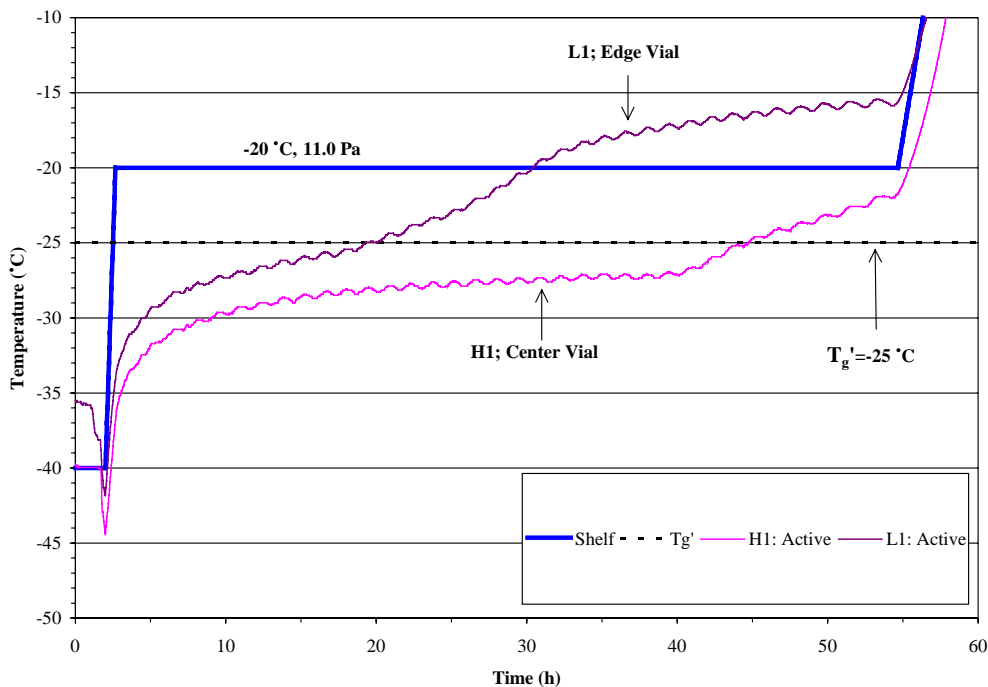


Fig. 12. Pocket logger thermistor (product) temperature during primary drying for the demonstration run (Trial 4) in manufacturing at final set points.

± 1.5 Pa) to ensure complete primary drying for all product vials within the 52 h step duration and keep the ice temperature below the glass transition temperature of -25 °C. The simulation results in Figs. 9–11 showed that the most influential operating parameter for heat transfer to the product vials was the shelf temperature with chamber pressure having a lesser effect.

Figs. 12 and 13 show representative product temperature trends from Trial 4 (demonstration run) shelf center and edge vials during primary and secondary drying, respectively. Fig. 12 shows that all vials completed primary drying well in advance of the completion of the step, demonstrated by the trend of the center vial (vial H1). The temperature of the frozen solution of center vial H1 started to rise faster after ~ 38 h, indicating completion of primary drying at about 38–40 h. The experimental completion of primary drying is in good agreement with the theoretical predictions in Fig. 11. The duration for primary drying was predicted to be ~ 41 h, when adjusted for a fill volume of 5.8 ml. Fig. 13 shows the secondary drying product temperature trends for the same vials. As

with the earlier scale-up batches, center vials attained higher temperature than edge vials during secondary drying. The moisture results from the demonstration run are shown in Fig. 8, with an average value of 1.6%, in line with the other scale-up trials. The product had no visible signs of collapse, and met all physical and chemical product specification attributes.

4.4. Pilot plant versus manufacturing lyophilizers

Fig. 8 moisture results showed that the product from manufacturing had lower moisture from the pilot plant batches despite the similarity of the lyophilization cycles applied at the two facilities. Therefore, an experimental active batch was manufactured in the pilot plant and the product temperature was monitored using Pocket Loggers, as was done in manufacturing. The product temperature results from secondary drying are shown in Fig. 14, and show that the product temperature during the two steps of secondary drying in the pilot plant unit was lower than that attained in a manufacturing lyophilizer. The difference is at-

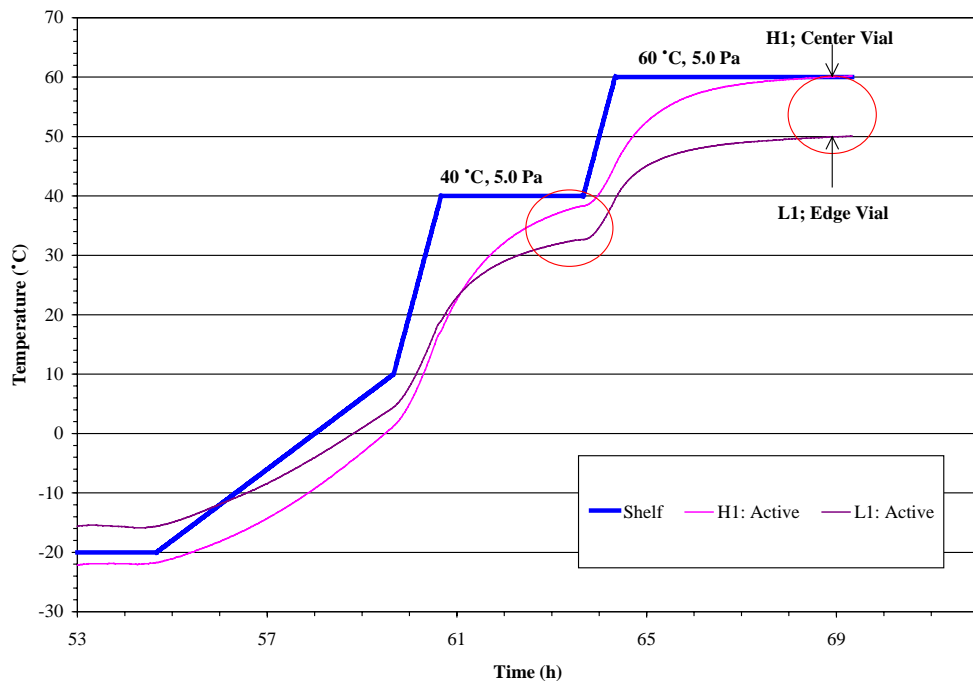


Fig. 13. Pocket logger thermistor (product) temperature during secondary drying for the demonstration run (Trial 4) in manufacturing at final set points.

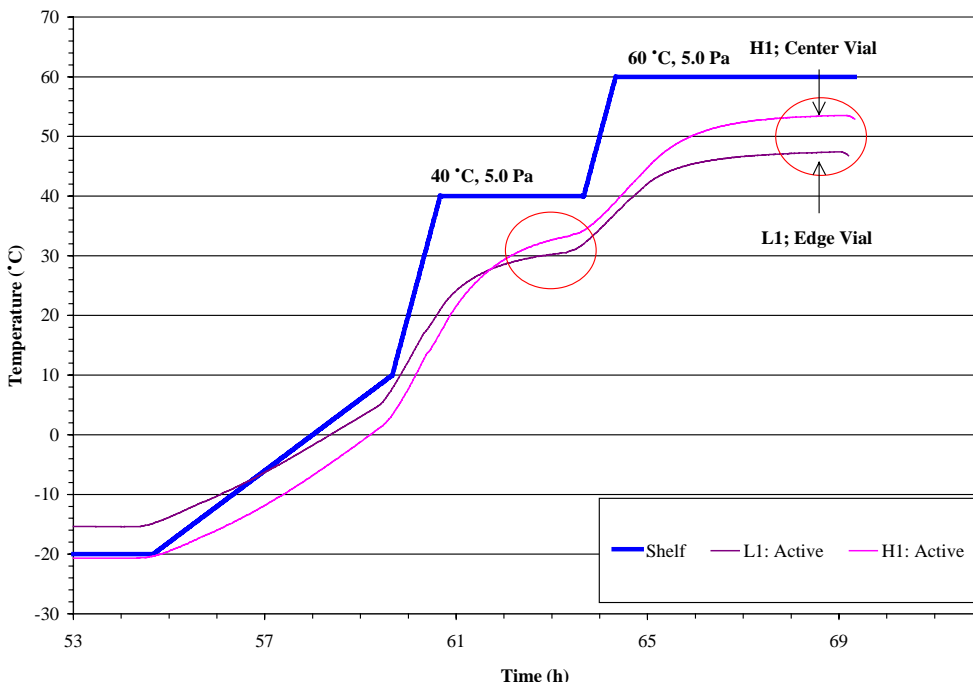


Fig. 14. Pocket logger thermistor (product) temperature during secondary drying for a batch manufactured in the pilot plant at final set points.

tributed to different heat transfer characteristics of the lyophilizers, with the manufacturing lyophilizer in the present case having a 'more efficient' heat transfer coefficient than the pilot plant unit at secondary drying conditions. Such differences between lyophilizers of different scales are case-specific and can not be known a priori. The above results underscore the importance of accounting for different heat transfer characteristics of lyophilizer units as the product is moved through development to manufacturing. Freeze drying cycle transfer must be based on equivalent drying rates and extent of drying at the different scales, especially when product final moisture content is critical. This could be achieved by following the drying process using product temperature (or by monitoring the moisture content of the effluent gas from the lyophilizer chamber to the condenser) during the development and technical transfer activities. Scaling-up shelf temperature and chamber pressure set points might not be sufficient, since different units can have different heat characteristics, irrespective of size, thus yielding different rates of heat transfer to the product.

5. Conclusions

Appropriate scale-up of a freeze drying process in a cost effective and efficient manner involves smart use of experimental tools to monitor the drying process of product in limited experiments at manufacturing conditions. Use of modeling can tremendously enhance the possibility of success by evaluating the robustness of the developed manufacturing cycle around target set points. In this manuscript the methodology for scaling-up and transferring a lyophilization process of a labile pharmaceutical product from pilot plant to manufacturing was described. Experimental data were collected during limited scale-up trials in manufacturing using Pocket Loggers to determine the lyophilization set points and process operating ranges. The experimental data were used to calculate the appropriate heat transfer coefficients of manufacturing lyophilizers using a single-vial freeze drying model. The model was then used to evaluate the robustness of the lyophilization cycle at different operating conditions, including changes in shelf temperature, chamber pressure, and vial fill volume. Based on the combined experimental and theoretical work, the freeze drying

cycle at manufacturing was determined and demonstrated experimentally. Freeze drying cycle scale-up must be based on equivalent drying rates and extent of drying at the different scales. Monitoring product temperature inside the lyophilizers during development and technical transfer activities is one methodology to ensure successful scale-up. Scaling-up shelf temperature and chamber pressure set-points may not be adequate, since different units might have different heat characteristics, irrespective of size, thus yielding different rates of heat transfer to the product.

Acknowledgements

The successful transfer of the lyophilization cycle of this product to manufacturing would not have been possible without the close collaboration between the Pharmaceutical R&D and Manufacturing Technical Teams. Especially, we would like to thank A. Kanike and K. Illig of Pharmaceutical Development for their early participation in the process development efforts. We thank J. Bak of Manufacturing Validation for suggesting the possible use of Pocket Loggers during the technical transfer of the lyophilization cycle to the manufacturing units. In addition, the following colleagues, K. Ford and D. Cross (Pharmaceutical Development), M. Akar, P. Coppens, R. Hanes, D. Long, D. O'Connell, A. Orella, and B. Phillips (Manufacturing Technical Operations) were invaluable for their participation and efforts in the planning of scale-up activities and collecting the thermal data.

References

- FDA Guideline on General Principles of Process Validation, May 1987. Current Good Manufacturing Practices Regulations for Finished Pharmaceuticals. 21 CFR Parts 210 and 211.
- Franks, F., 1990. Freeze-drying: from empiricism to predictability. *Cryo-Lett.* 11, 93–110.
- Liapis, A.I., Bruttini, R., 1994. A Theory for the primary and secondary drying stages of the freeze-drying of pharmaceutical crystalline and amorphous solutes: comparison between experimental data and theory. *Separat. Technol.* 4, 144–155.
- Liapis, A.I., Bruttini, R., 1995. Freeze-drying of pharmaceutical crystalline and amorphous solutes in vials: dynamic multi-dimensional models of the primary and secondary drying stages and qualitative features of the moving interface. *Drying Technol.* 13, 43–72.

Liapis, A.I., Pikal, M.J., Bruttini, R., 1996. Research and development needs and opportunities in freeze drying. *Drying Technol.* 14, 1265–1300.

MacKenzie, A.P., 1975. Collapse during freeze drying—qualitative and quantitative aspects. In: Goldblith, S.A., Rey, L., Rothmayr, W.W. (Eds.), *Freeze Drying and Advanced Food Technology*. Academic Press, London, pp. 277–307.

Nail, S.L., Gatlin, G.A., 1992. Freeze drying: principles and practice. In: Avis, K.E., Lieberman, H.A., Lachman, L. (Eds.), *Pharmaceutical Dosage forms: Parenteral Medications*, vol. 2, Marcell Dekker Inc., New York, pp. 163–233.

Peters, M.S., Timmerhaus, K.D., 1981. *Plant Design and Economics for Chemical Engineers*. McGraw-Hill, Tokyo, pp. 635–637.

Pikal, M.J., Shah, S., Senior, D., Lang, J.E., 1983a. Physical chemistry of freeze drying: measurement of sublimation rates for frozen aqueous solutions by a microbalance technique. *J. Pharm. Sci.* 72, 635–650.

Pikal, M.J., Roy, M.L., Shah, S., 1984. Heat and mass transfer in vial freeze drying of pharmaceuticals: role of the vial. *J. Pharm. Sci.* 73, 1224–1237.

Pikal, M.J., 1985. Use of laboratory data in freeze drying process design: heat and mass transfer coefficients and computer simulation of freeze drying. *J. Parent. Sci. Technol.* 39, 115–135.

Pikal, M.J., 1990a. Freeze drying of proteins. Part I: process design. *Biopharmaceutics* 3, 18–27.

Pikal, M.J., 1990b. Freeze drying of proteins. Part II: formulation selection. *Biopharmaceutics* 3, 26–30.

Pikal, M.J., Shah, S., Roy, M.L., Putman, R., 1990. The secondary drying stage of freeze drying: drying kinetics as a function of temperature and chamber pressure. *Int. J. Pharm.* 60, 203–217.

Sadikoglu, H., Liapis, A.I., 1997. Mathematical modelling of the primary and secondary drying stages of bulk solution. *Drying Technol.* 15, 791–810.

Rajniak, P., Placek, J., Reynolds, S.D., Hunke, W.A., 1999. Mathematical Modeling of Primary Drying. AAPS Annual Meeting, paper 2881, 14–18 November, New Orleans.

Rajniak, P., Placek, J., Tsinontides, S.C., Reynolds, S.D., 2000. In: *Proceedings of AIChE Annual Meeting, Mathematical Models for scale-up of Lyophilization*. Paper 284j, 16 November, Los Angeles.

Tsinontides, S.C., Pham, D., Rajniak, P., Hunke, W.A., Placek, J., Reynolds, S.D., 2001. In: *Proceedings of AIChE Annual Meeting, Lyophilization—From Pilot Plant to Manufacturing Using Theory and Experiment*. Paper 48g, 9 November, Reno.